Unusual η^1-Coordinated Alkyne and Alkene Complexes

Longfei Li,[a,c]* Mengxian Dong,[a] Hua-Jie Zhu,[a]*

Bin Peng,[b,c] Yaoming Xie,[c] Henry F. Schaefer III[c]*

[a] *College of Pharmacy, Hebei University, Baoding 071002, Hebei, P. R. of China*

[b]*MOE Key Laboratory of Theoretical Chemistry of the Environment, Center for Computational Quantum Chemistry, South China Normal University, Guangzhou, 510006, P. R. China*

[c] *Center for Computational Quantum Chemistry, University of Georgia, Athens, GA 30602, USA*

*Email: lilongfei@hbu.edu.cn (L.L.), zhuhuajie@hotmail.com (H.-J. Z.), ccq@uga.edu (H.F.S.)

Abstract

This mechanistic study demonstrates that an unusual η^1-coordinated alkyne complex is critical for the 1-pentyne 1,1-diboration reaction. The comparative studies suggest the "pull-push" antagonistic effect arising from Lewis acidity and steric congestion to be the reason for the existence of η^1-coordinated alkyne complex. Analogous η^1-coordinated alkene complexes are also predicted, and they are promising for applications to the important olefin polymerization reaction.

Introduction

The alkyne diboration reactions are important in organic synthesis, and used to yield versatile bis(boryl)alkene derivatives.[1] Since Miyaura and Suzuki discovered the platinum catalyzed alkyne 1,2-diboration in 1993,[2] a number of catalysts for this transformation have been developed.[3] These alkyne ligands adopt the η^2-coordination and the mechanism is rationalized by the *Dewar–Chatt–Duncanson* model.[4] In contrast, the alkyne 1,1-diboration has been rarely reported.[5] In 2015 Sawamura and coworkers realized the alkyne 1,1-diboralation, and Brønsted base was used to abstract the hydrogen of the terminal C(sp)-H in alkynes.[6] In 2017, Chirik and coworkers developed the cobalt-catalyzed 1,1-diboration of terminal alkynes, and the key C(sp)-H bond activation step proceeds via σ-bond metathesis.[7]

In 2018 Erker and coworkers reported a bulky diborane compound (structure **1** in Scheme 1).[8] At room temperature and in CD_2Cl_2 solvent, diborane **1** reacts with 1-pentyne to synthesize a mixture of the 1,1- and 1,2-diboration products (**2** and **3**) as the major components in the final ratio of 42:37 plus unidentified product (21%), although **3** was first observed[8] in the fractional crystallization experiments. Since this reaction proceeds in the absence of metal complex and Brønsted base, its mechanism must be different from that identified in previous cases. To gain a better understanding of the reactivities of alkynes, we have undertaken theoretical studies of the alkyne 1,1-diboration.

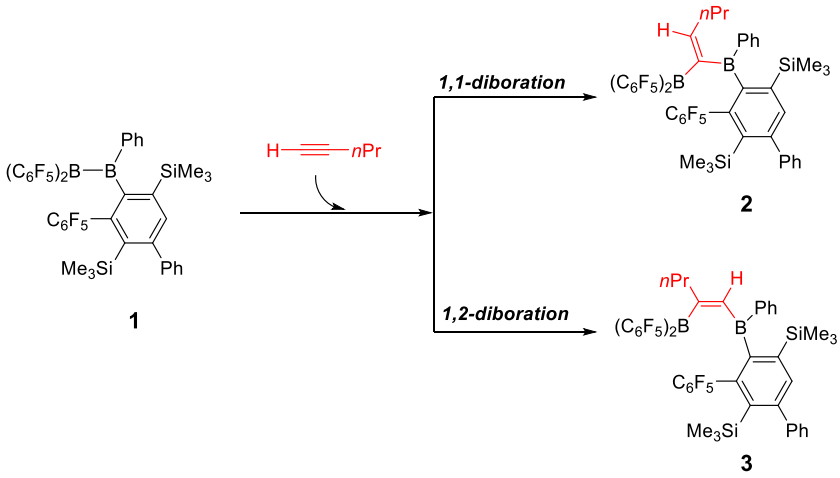

Scheme 1. The synthesis of 1,1- and 1,2-diboration of 1-pentyne by Erker and coworkers.[8]

Computational Methods

Our theoretical studies were carried out with the DFT ωB97X-D method[9] and the 6-31G(d,p) basis sets using the Gaussian 09 program.[10] The geometries were optimized in dichloromethane solution, and the solvent effects were evaluated using the SMD (Solution Model based on Density) method.[11] Thermal corrections and entropy contributions to the Gibbs free energy were taken from frequency computations with the same ωB97X-D/6-31G(d,p) level of theory in dichloromethane solution. All transition states were confirmed to exhibit only one imaginary vibrational frequency via Hessian analyses. We have thoroughly examined the conformational space of each intermediate and transition state, and the lowest energy conformers are included in the discussions. Natural bond orbital (NBO) analyses were performed using NBO 6.0 program.[12]

In order to confirm the DFT predictions, single point energies with the larger 6-311G(2d,2p) basis set were evaluated with key structures. We also employed newer density functionals (MN15, B3LYP-D3, M06-2X) to study the reaction pathways. Since all the methods predict consistent results, we only discuss the ωB97X-D/6-31G(d,p) results in the text, while the other results are reported in Supporting Information (SI).

Results and discussion

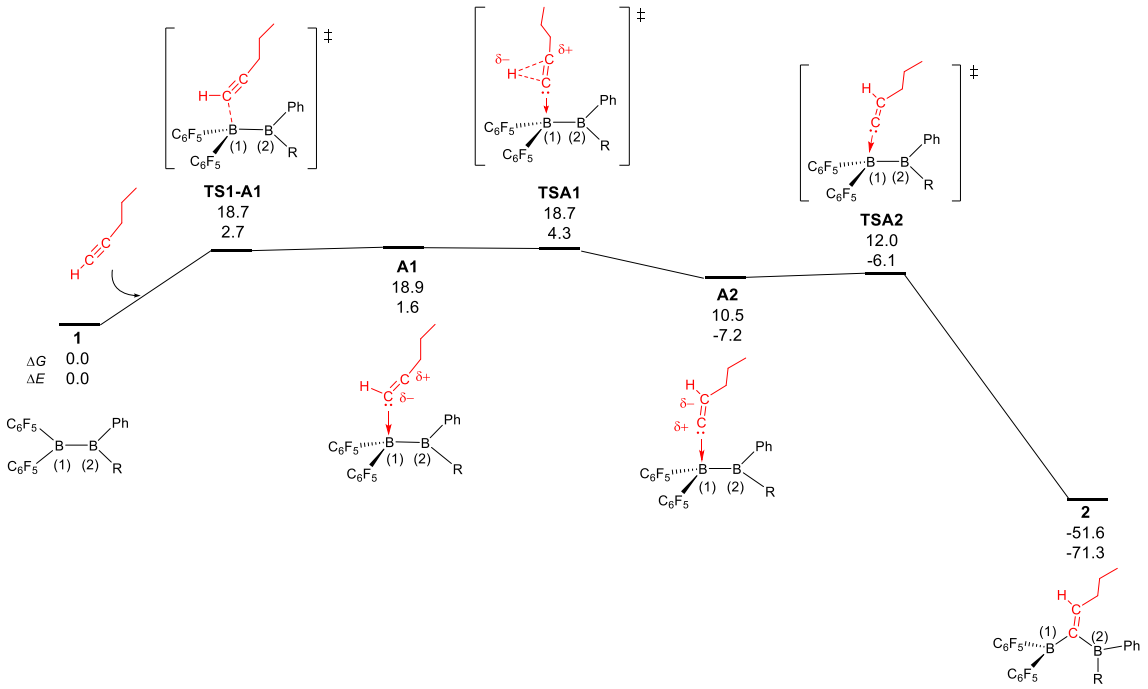

Figure 1. Gibbs free energy profiles (in kcal/mol) for the 1,1-diboration pathway of Scheme 1. R signifies the pentasubstituted phenyl ring.

The 1,1-diboration pathway is illustrated in Figure 1. Therein, the 1-pentyne can coordinate with the B(1) atom in diborane **1** through the transition state **TS1-A1**. The unusual

η^1-coordinatied structure **A1** with an energy of 18.9 kcal/mol above **1** is found. However, the common η^2-coordinatied structure was not located, because it collapses to the η^1-coordinatied structure. The geometry of **A1** is reported in Figure 2. The C(2)-B(1) separation (2.756 Å) is significantly longer than the C(1)-B(1) bond (1.766 Å), and the former is too long to describe as a conventional bond. The angles H(1)-C(1)-C(2), B(1)-C(1)-C(2), B(1)-C(1)-H(1) are 120°, 131°, 108°, respectively, indicating the approximate sp^2 hybridization of the C(1) atom. In contrast, atom C(2) remains approximately sp hybridized due to the near linear arrangement of C(1)-C(2)-C(3) (178°). Therefore, it may be concluded that 1-pentyne adopts an unusual η^1 terminal coordination mode with respect to the diborane.

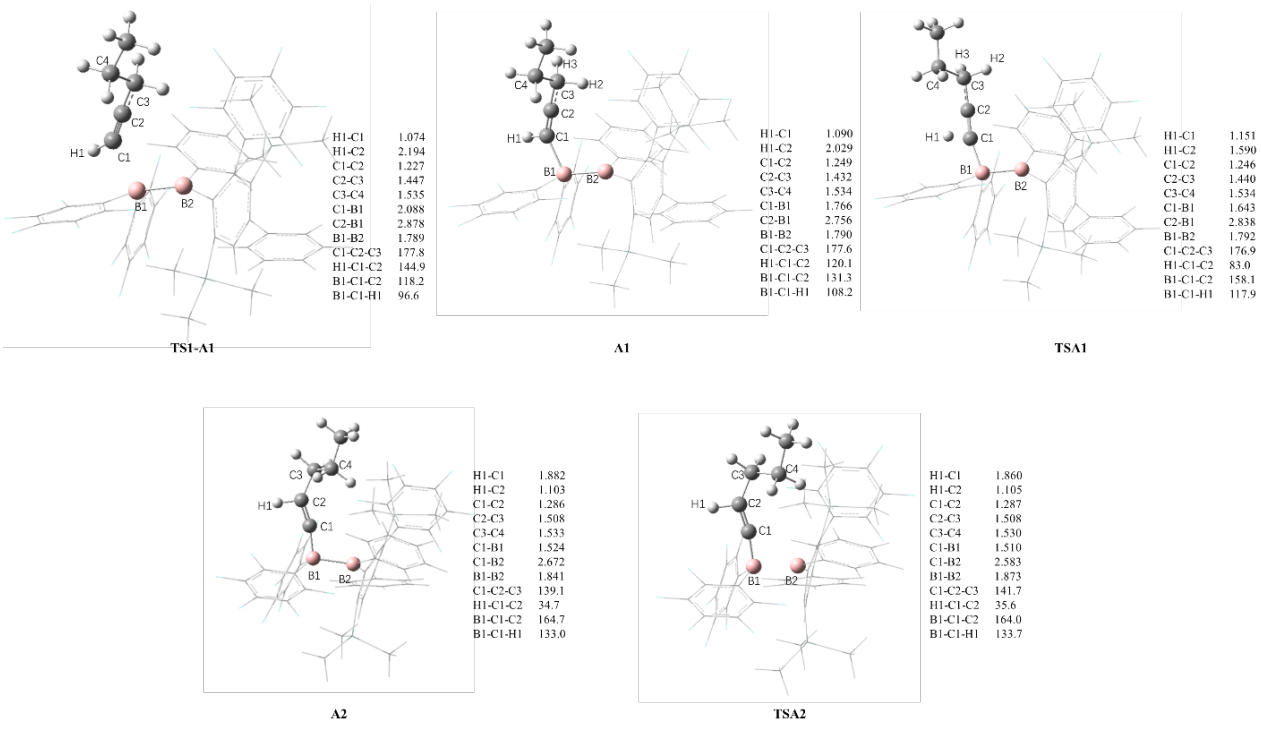

Figure 2. The structures in the 1,2-diboration pathway. The internuclear separations are in Å. The groups on the B atoms are drawn in wireframe for simplicity. However, all atoms were included in the geometry optimization.

The electronic structure for the complex **A1** with an η^1-1-pentyne fragment has been studied via NBO analysis. The 1-pentyne moiety is bonded to diborane via one C atom of the C≡C bond, by donating two π electrons of C≡C into the empty *p* orbital of the B(1) atom to form a C(1)-B(1) bond, leaving the C(2) atom electron-deficient. The NBO analysis showed a "lone vacancy" (LV) for the C(2) atom, which corresponds to an empty valence-p orbital (p_{C2}* is used below). Accordingly, the natural atomic charges for C(1) and C(2) are -0.45 and +0.42, respectively. The NBO second-order perturbation stabilizing energies *E*(2) for the $\sigma_{C1\text{-}B1} \rightarrow p_{C2}$*, $\sigma_{C1\text{-}H1} \rightarrow p_{C2}$*, $\sigma_{C3\text{-}H3} \rightarrow p_{C2}$*, $\sigma_{C3\text{-}H4} \rightarrow p_{C2}$* electron transfer are estimated as 59, 33, 14, and 23 kcal/mol, respectively. These may provide a measure for the hyperconjugation effects. In Figure 3 the electron density of C-H and C-B bonds near the C(2) atom delocalize to the empty p_{C2}* orbital. The hyperconjugation interactions lead to a shorter C(2)-C(3) bond (1.432 Å) in **A1**, compared to that in free 1-pentyne (1.464 Å). In addition, the transfers of $\sigma_{C3\text{-}H3} \rightarrow \sigma_{C1\text{-}C2}$* (3.9 kcal/mol) and $\sigma_{C3\text{-}H2} \rightarrow \sigma_{C1\text{-}C2}$* (4.0 kcal/mol) have also made minor contribution to the hyperconjugation effects. The NBO analysis shows no significant donation from the C(1)-H(1) bond to the B(1) atom. The NRT computations for the simplified model of **A1** showed that the weight of the resonance structure with agostic C(1)-H(1) to B(1) atom is very low (1.1%), while the structure **A1** displayed in Figure 3 has the largest weight (47%).

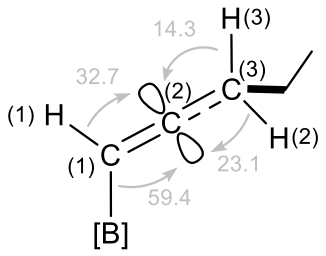

Figure 3. Schematic representations of hyperconjugation in the coordinated 1-pentyne compound. The numerical results are the NBO second-order perturbation stabilizing energies *E*(2) in kcal/mol.

Since the C(1)-H(1) bond is largely activated in association with the strong $\sigma_{C1\text{-}H1} \rightarrow p_{C2}^*$ hyperconjugation effect, the H(1) atom could move across the C(1)-C(2) bond with a small energy barrier. Although the total energy (ΔE) of **TSA1** is higher than **A1** by 2.7 kcal/mol, the Gibbs free energy (ΔG) for transition state **TSA1** is 0.2 kcal/mol lower than that of **A1**. In the subsequent steps, the intermediate **A2,** with a Gibbs free energy of 10.5 kcal/mol above **1**, is generated, and the NPA charges for the C(1), C(2), B(1), B(2) atoms are +0.25, -0.32, -0.06, +0.82, respectively. The subsequent transfer of carbon atom C(1) between B(1) and B(2) atoms will lead to the cleavage of the B(1)-B(2) bond. As a result, the 1,1-diboration product **2** is formed with a large exergonic reaction energy of 52 kcal/mol. In brief, the formation of the η^1-coordination complex **A1** allows the C(sp)-H cleavage and further leads to the unusual 1,1-diboration product.

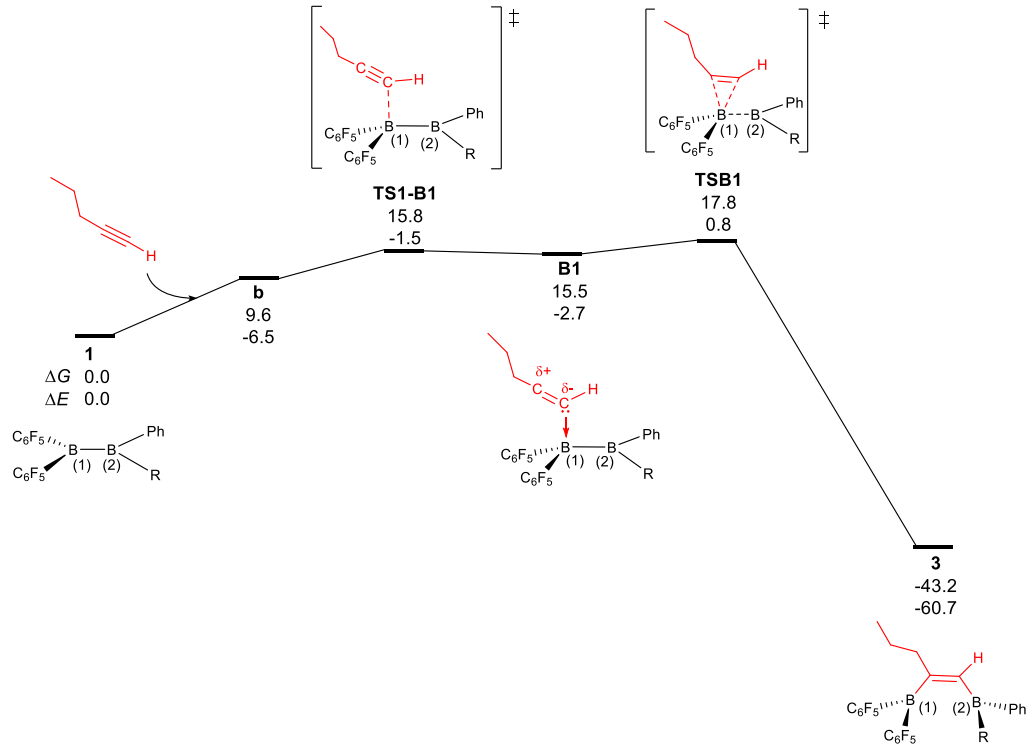

Figure 4. Gibbs free energy profiles (in kcal/mol) for the 1,2-diboration pathway. R denotes the pentasubstituted phenyl ring.

In the 1,2-diboration pathway (Figure 4), 1-pentyne can match the pocket of diborane **1**, generating a supramolecular intermediate **b** through a non-convalent interaction with a free energy of 9.6 kcal/mol, and the three-dimension figure of **b** is reported in Figure 5. The bounded 1-pentyne can further approach the B(1) atom in another η^1-coordination motif through the transition state **TS1-B1**. Compared with its isomer **A1** (for the 1,1-diboration in Figure 1), **B1** has less steric hindrance, and it could lie in lower energy. In fact, the free energy of **B1** is 15.5 kcal/mol above **1**, which is 3 kcal/mol lower than **A1**. Nevertheless, the coordinated 1-pentyne in **B1** bears the same electronic structure as in **A1** according to the analysis in Figure S1 in SI. The shift of carbon atom C(1) from the B(1) atom to B(2) will lead to a cleavage of the

B-B bond, and this requires the system to overcome an energy barrier of 2 kcal/mol. In the transition state **TSB1**, both the carbon atoms in the C(1)≡C(2) moiety are linked to the B(1) atom. As shown in Figure 5, the C(1)-B(1) and C(2)-B(1) distances are 1.760 and 1.942 Å, respectively, suggesting an η^2-coordination structure for 1-pentyne with diborane. After passing the barrier, the 1,2-diboration product **3** is generated, with a relative Gibbs free energy of -43 kcal/mol. In comparison with the 1,1-diboration pathway (Figure 1), the barrier for the transition state **TSB1** is 0.9 kcal/mol lower than **TSA1**, but the corresponding product **3** is higher than the product **2** by 8 kcal/mol. Our theoretical results agree well with experiment that the 1,2-diboration product **3** is formed first during the fractional crystallization, while the amounts of the 1,1-diboration product **2** increases subsequently. The final ratio of products **2** and **3** becomes 42:37, since the product **2** is favored under thermodynamical control.

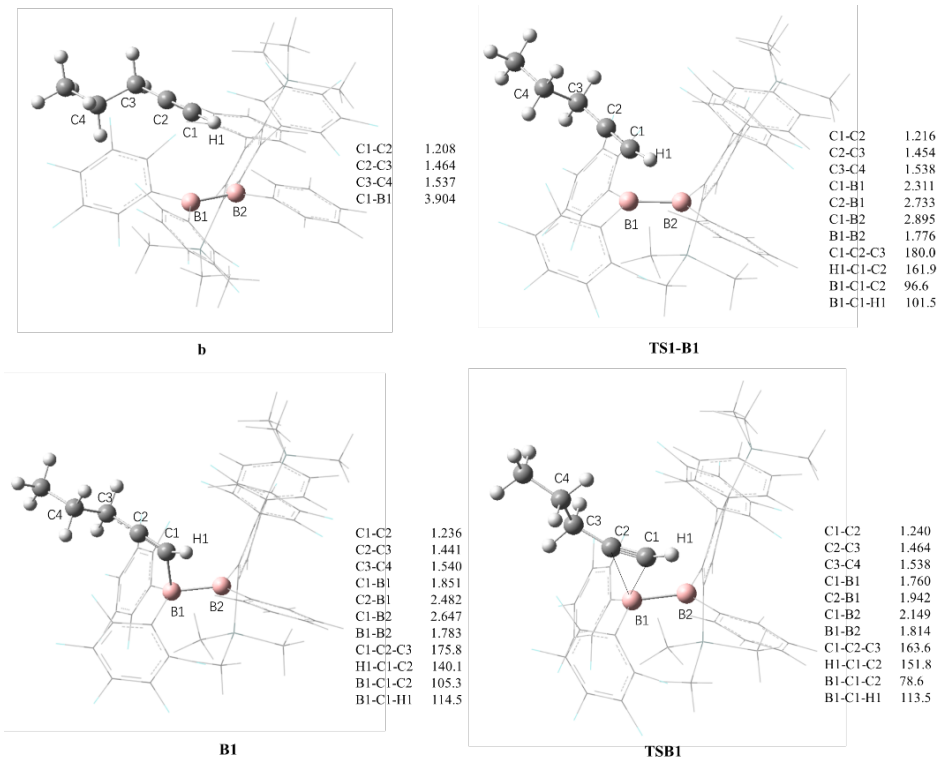

Figure 5. The structures in the 1,2-diboration pathway. The internuclear separations are in Å. The groups on the B atoms are drawn in wireframe for simplicity. However, all atoms were included in the geometry optimization.

In order to gain insight into the origins of the η^1-coordinatied alkyne complexes, two comparable studies are performed. When the strongly electrophilic -C_6F_5 groups in the diborane **1** (Figure 1) are modulated into the -C_6H_5 group, the presumptive η^1-coordinatied structures **A1_a** and **B1_a** (Figure 6), bearing same steric congestion with **A1** and **B1** respectively, could not be located in the optimization. This is because the alkyne will dissociate from the B(1) center, which implies that the Lewis acidity of diboranes **A1_a** and **B1_a** is not strong enough to "pull" the alkynes. When the -Ph and pentasubstituted phenyl rings in the diborane **1** are modulated into the small -Me groups, the presumptive η^1-coordinatied structure **A1_b** (Figure 6)

is not a local minimal, and the concerted alkyne η^2-coordination and alkyne 1,2-insertion steps take place. This is different from the 1,1-diboration (in Figure 1) from **A1** to **2**, in which there is a large steric hindrance of the pentasubstituted phenyl ring on B(2) atom. The result demonstrates that diborane must retain sufficient steric bulk to "push" the alkyne fragment and hence precludes the classical η^2-coordination of alkynes. In brief, the "pull-push" antagonistic interaction, which stems from the Lewis acidity and steric congestion of boranes, is the origin for the η^1-coordinatied alkyne complexes. With the "pull-push" antagonistic interaction as the guiding principle, we have devised a series of η^1-coordinatied alkyne complexes (Figure S6 – S9), which enable -H, -CH_3, -C_2H_5, and -SiH_3 groups to transfer across the C-C bond of alkyne motif to achieve thermally induced 1,1-diboration reactions.

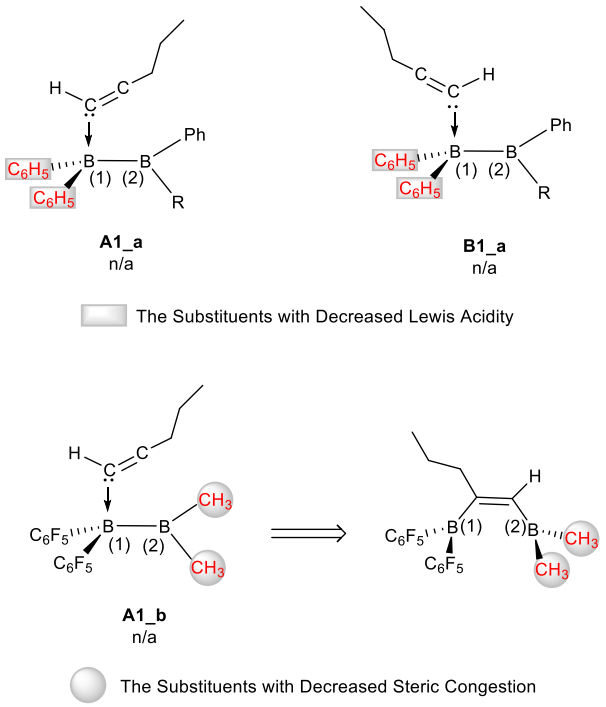

Figure 6. The presumptive η^1-coordinatied alkynes complexes with different substituents. R denotes the pentasubstituted phenyl ring.

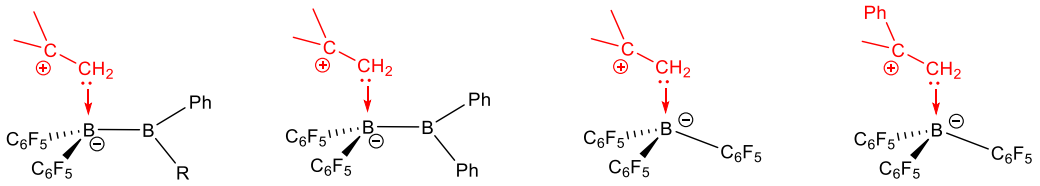

Figure 7. The designed η^1-coordinatied alkynes complexes. The energies (both ΔG and ΔE) are computed at the ωB97X-D/6-31G(d, p) level.

Interestingly, we found alkenes can also form analogous η^1-coordinatied complexes. Meeting the requirement of the "pull-push" antagonistic interaction, the boranes, such as $(C_6F_5)_2$B-BPhR and B$(C_6F_5)_3$ bearing bulky and electron-withdrawing C_6F_5 groups, can bind the alkenes to form η^1-coordinatied structures as shown in Figure 7. The η^1-coordinatied alkene complexes are characterized by zwitterionic structures, and the reactive carbocation should be available for further nucleophilic reactions. This prompted us to explore the possible application of this kind of complexes. In this respect, the η^1-coordinatied alkene complex **D1** (Figure 8) was designed with strong electron-attracting -CF_3 groups, and it has a much lower energy (17.4 kcal/mol below the reactants, Figure 8) because of the stronger Lewis acid B$(CF_3)_3$ forming a strong B$(CF_3)_3$-alkyne bond. The complex **D1** has the potential to undergo the nucleophilic addition through the transition state **TSD1-2** with an energy barrier of 9.6 kcal/mol. The following chain propagation proceeds through repetitive nucleophilic additions that are thermodynamically downhill with low energy barriers. The conversion from **D2** to **D3** proceed

with no barrier, and the energy scan is shown in Figure S1 in Supporting Information. It is envisioned that a polypropylene macromolecule will be found in the end, which may provide unique metal-free routes to the industrially important alkene polymerization.

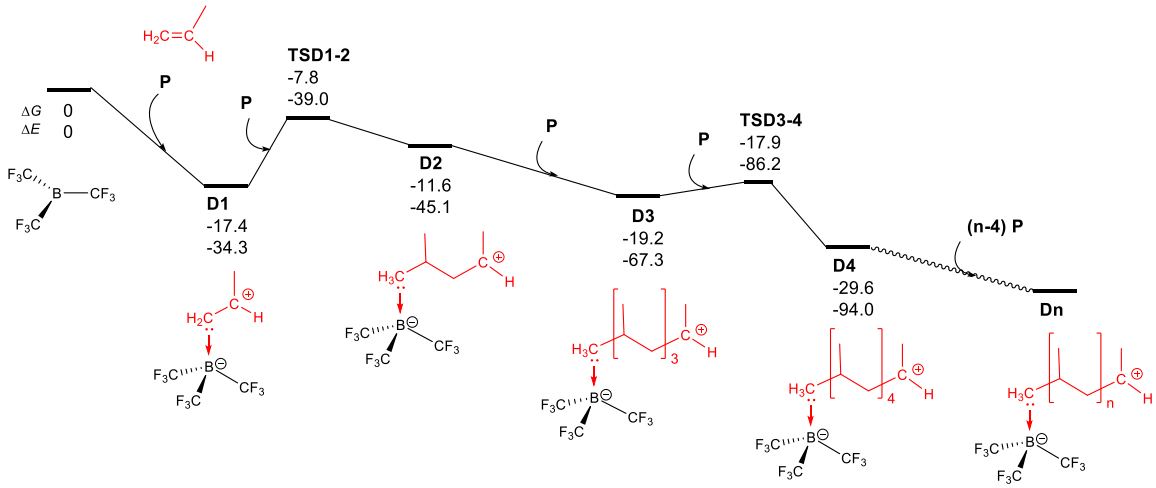

Figure 8. Designed olefin polymerization initiated by η^1-coordinatied alkene complexes. The energies (both ΔG and ΔE) are computed at the ωB97X-D/6-31G(d, p) level. The symbol P denotes the propylene.

Conclusions

In summary, the present theoretical study suggests that the η^1-coordinated alkyne complex **A1** are crucial for the unusual alkyne 1,1-diboration reactivity. The comparable studies the suggest the "pull-push" antagonistic interaction attributed to the Lewis acidity and steric congestion of boranes is the origin for the unusual η^1-coordinated alkyne complexes. From this perspective, we have designed a series of the η^1-coordinated alkyne complexes which enable -H, -CH_3, -C_2H_5, and -SiH_3 groups to transfer across C-C bonds of alkyne motif to

achieve thermally induced 1,1-elementoboration reactions. Interestingly, we found the unprecedented η^1-coordinated alkene complexes, and further computationally design shows that these complexes may initiate the propylene polymerization and open up efficient metal-free routes for industrially important polyolefin reactions. The study leads to the important conclusion that carbon-carbon double and triple bonds can adopt the unusual η^1-coordination mode. We hope our results will stimulate the further experimental studies on the possible reactivity and utility of η^1-coordinated alkyne/alkene complexes.

ASSOCIATED CONTENT

Supporting Information

The optimized geometries and energies of all stationary points along the reaction pathways, as well as the imaginary frequencies of transition states.

Notes

The authors declare no competing financial interest.

ACKNOWLEDGMENTS

This work was supported by the National Natural Science Foundation of China (No. 21903018，21877025), the Natural Science Foundation of Hebei Province of China (No. B2019201128). The research at the Center for Computational Quantum Chemistry was supported by National

Science Foundation (CHE 1661604). We thank the High Performance Computer Center of Hebei University for providing the computational resources.

References

[1] a) S. J. Lee, K. C. Gray, J. S. Paek and M. D. Burke, *J. Am. Chem. Soc.* **2008**, *130*, 466-468; b) M. Shimizu, I. Nagao, Y. Tomioka and T. Hiyama, *Angew. Chem. Int. Ed. Engl.* **2008**, *47*, 8096-8099; c) R. Barbeyron, E. Benedetti, J. Cossy, J.-J. Vasseur, S. Arseniyadis and M. Smietana, *Tetrahedron* **2014**, *70*, 8431-8452.

[2] T. Ishiyama, N. Matsuda, N. Miyaura and A. Suzuki, *J. Am. Chem. Soc.* **1993**, *115*, 11018-11019.

[3] a) S. G. Curto, M. A. Esteruelas, M. Oliván, E. Oñate and A. Vélez, *Organometallics* **2018**, *37*, 1970-1978; b) H.-Y. Jung and J. Yun, *Org. Lett.* **2012**, *14*, 2606-2609.

[4] a) G. Bistoni, P. Belanzoni, L. Belpassi and F. Tarantelli, *J. Phys. Chem. A* **2016**, *120*, 5239-5247; b) M. De Santis, S. Rampino, H. M. Quiney, L. Belpassi and L. Storchi, *J. Chem. Theory Comput.* **2018**, *14*, 1286-1296; c) L. Triguero, A. Föhlisch, P. Väterlein, J. Hasselström, M. Weinelt, L. G. M. Pettersson, Y. Luo, H. Ågren and A. Nilsson, *J. Am. Chem. Soc.* **2000**, *122*, 12310-12316; d) F. Bauer, H. Braunschweig, K. Gruss and T. Kupfer, *Organometallics* **2011**, *30*, 2869-2884; e) C. Kojima, K.-H. Lee, Z. Lin and M. Yamashita, *J. Am. Chem. Soc.* **2016**, *138*, 6662-6669.

[5] E. C. Neeve, S. J. Geier, I. A. Mkhalid, S. A. Westcott and T. B. Marder, *Chem. Rev.* **2016**, *116*, 9091-9161.

[6] A. Morinaga, K. Nagao, H. Ohmiya and M. Sawamura, *Angew.Chem. Int.Ed.* **2015**, *54*, 15859-15862.

[7] S. Krautwald, M. J. Bezdek and P. J. Chirik, *J. Am. Chem. Soc.* **2017**, *139*, 3868-3875.

[8] F. Ge, X. Tao, C. G. Daniliuc, G. Kehr and G. Erker, *Angew.Chem. Int.Ed.* **2018**, *57*, 14570-14574.

[9] J.-D. Chai and M. Head-Gordon, *Phys. Chem. Chem. Phys.* **2008**, *10*, 6615-6620.

[10] M. J. Frisch, G. W. Trucks, H. B. Schlegel, G. E. Scuseria, M. A. Robb, J. R. Cheeseman, G. Scalmani, V. Barone, B. Mennucci, G. A. Petersson, H. Nakatsuji, M. Caricato, X. Li, H. P. Hratchian, A. F. Izmaylov, J. Bloino, G. Zheng, J. L. Sonnenberg, M. Hada, M. Ehara, K. Toyota, R. Fukuda, J. Hasegawa, M. Ishida, T. Nakajima, Y. Honda, O. Kitao, H. Nakai, T. Vreven, J. J. A. Montgomery, J. E. Peralta, F. Ogliaro, M. Bearpark, J. J. Heyd, E. Brothers, K. N. Kudin, V. N. Staroverov, T. Keith, R. Kobayashi, J. Normand, K. Raghavachari, A. Rendell, J. C. Burant, S. S. Iyengar, J. Tomasi, M. Cossi, N. Rega, J. M. Millam, M. Klene, J. E. Knox, J. B. Cross, V. Bakken, C. Adamo, J. Jaramillo, R. Gomperts, R. E. Stratmann, O. Yazyev, A. J. Austin, R. Cammi, C. Pomelli, J. W. Ochterski, R. L. Martin, K. Morokuma, V. G. Zakrzewski, G. A. Voth, P. Salvador, J. J. Dannenberg, S. Dapprich, A. D. Daniels, O. Farkas, J. B. Foresman, J. V. Ortiz, J. Cioslowski and D. J. Fox, GAUSSIAN 09, Gaussian, Inc., Wallingford CT, 2009..

[11] a) A. V. Marenich, C. J. Cramer and D. G. Truhlar, *J. Phys. Chem. B.* **2009**, *113*, 6378-6396; b) J. Tomasi and M. Persico, *Chem. Rev.* **1994**, *94*, 2027-2094.

[12] E. Glendening, A. Reed, J. Carpenter, F. Weinhold, NBO Version 3.1, TCI. NBO 3.1 program 1998, 65.

TOC Graphic:

η^1-Coordinated Alkyne and Alkene Complexes